Research Article

Israel Journal of Chemistry
www.ijc.wiley-vch.de

doi.org/10.1002/ijch.202100126

1,7-Diazaperylene in Organic Field Effect Transistors

Cigdem Yumusak,[a, b] Felix Mayr,[a, c] Dominik Wielend,[a] Bilge Kahraman,[a, d] Yasin Kanbur,[a, e] Heinz Langhals,[f] and Mihai Irimia-Vladu*[a]

Dedicated to Prof. Niyazi Serdar Sariciftci on the occasion of his 60th birthday.

Abstract: A thorough material characterization of 1,7-diazaperylene via multiple investigation techniques (cyclic voltammetry, photoluminescence, photoluminescence excitation, impedance spectroscopy) was performed to understand its applicability in organic electronic devices. The recorded data of this perylene derivative was placed in conjunction with the respective data of the parent perylene molecule, and the behavior of this novel compound in organic electronic devices (planar diodes and field effect transistors explained). Although no photovoltaic effect behavior was recorded in planar diodes where 1,7-diazaperylene was employed both as a donor as well as an acceptor, the perylene derivatives proves functional as dielectric layer in organic field effect transistors.

Keywords: organic field effect transistor · dielectric capping layer · diazaperylene · perylene derivative

Introduction

Aromatic systems with electron-deficient moieties have attracted interest from the scientific community since they act as electron acceptors in organic photovoltaic applications.[1] Among them, 1,7-diazaperylene (benz[de]isoquino[1,8-gh]quinoline), CAS RN 85903 s97-5)[2] has been so far the focus of several investigations because of its high fluorescence quantum yield (*i.e.* ~83%) and substantial chemical and photochemical stability.[3–13] The electron withdrawing effect of the two nitrogen atoms stabilizes chemically the heterocycle compared with the parent hydrocarbon perylene. The planarity of 1,7-diazaperylene in contrast to the twisted geometry of the latter allows a more densely packing in solids as is shown by comparing the x-ray crystal structures of the two.[3] In fact, heteroaromatic molecules that are planar are densely packed, with density of about 1.4 g/cm^3, arranging themselves in a modified herringbone structure.[14] These special properties make this heterocyclic compound interesting for applications in material chemistry where claims such as in LED devices[15,16] were described. However, the inefficient synthesis of 1,7-diazaperylene limited both its technical usefulness and further research. The first described synthesis[2] required a very large excesses of Raney nickel, while a subsequent description[17] required comparably complicated reaction conditions not convenient for the preparation of larger quantities. On the other hand, a recently reported efficient synthetic method[14] suitable for upscaling was described where simple bulk chemicals were applied. This prompted us for further investigation and we looked into finding an applicability of this compound in organic electronic devices, *i.e.* organic field effect transistors and solar cells respectively. We have put the performance of 1,7-diazaperylene in context of the well-established cousin molecule perylene, and pursued the fabrication of organic photovoltaic devices and field effect transistors with this perylene derivative as active layer. As will be seen in the data presented here, we finally focused our attention into OFETs fabrication where 1,7-diazaperylene seems most suited. As a dielectric layer the impedance of diazaperylene was measured and n- (fullerene) and p-type (pentacene) transistors were fabricated. The results show the successful use of diazaperylene in organic electronic devices.

[a] *C. Yumusak, F. Mayr, D. Wielend, B. Kahraman, Y. Kanbur, M. Irimia-Vladu*
Johannes Kepler University Linz, Institute of Physical Chemistry, Linz Institute for Organic Solar Cells (LIOS), Altenberger Str. Nr. 69, 4040, Linz, Austria
E-mail: Mihai.Irimia-Vladu@jku.at
[b] *C. Yumusak*
Brno University of Technology, Faculty of Chemistry, Materials Research Centre, Purkyňova 118, 612 00, Brno, Czech Republic
[c] *F. Mayr*
Institute of Applied Physics, Johannes Kepler University Linz, Altenberger Str. 69, 4040 Linz, Austria
[d] *B. Kahraman*
Department of Material Science and Nanotechnology Engineering, TOBB ETU University, Söğütözü, Söğütözü Cd. No:43, 06510 Çankaya/Ankara Turkey
[e] *Y. Kanbur*
Department of Chemistry, Karabük University, Baliklarkayasi Mevkii, 78050 Karabük, Turkey
[f] *Prof. H. Langhals*
Department of Chemistry, LMU University of Munich, Butenandtstr. 13, D-81377 Münich, Germany

Experimental

Cyclic Voltammetry

Cyclic voltammetry (CV) was performed using an IPS-Jaissle Potentiostat/Galvanostat PGU10V-100 mA inside a nitrogen (N_2) flushed glove box. As electrochemical cell, a one-compartment cell with a 2 mm platinum (Pt) disc-type electrode (PalmSens) as working electrode, a platinum counter electrode and an Ag/AgCl electrode as quasi-reference electrode was used. The material investigated was weighed into the vial outside the glove box, transferred into the glove box where the according amount of electrolyte solution consisting of 0.1 tetrabutylammonium hexafluorophosphate ($TBAPF_6$, >99.0%, Sigma Aldrich) in acetonitrile (MeCN, >99.9%, Roth) was added to achieve a concentration of 0.5 mM. The CV scans were performed at a scan rate of 200 $mV\,s^{-1}$. In order to convert the applied potential versus the standard hydrogen electrode (SHE), after the measurement, a calibration with ferrocene (98%, Sigma Aldrich) was performed and the re-calculation done according to the literature[18] value of the ferrocene potential $E_{1/2=}+0.640$ V vs. SHE.

Spectroscopic Characterization

UV/Vis absorbance spectra were recorded on a PerkinElmer Lambda 1050 spectrophotometer. Photoluminescence (PL) and photoluminescence excitation (PLE) spectra were recorded on a Photon Technology International Quanta Master 40 spectrofluorometer with a dual monochromator arrangement in both the excitation and the emission channel, respectively. PL spectra were measured at an excitation wavelength of 400 nm, while PLE spectra were measured at the wavelength of the emission maximum of the corresponding material. For the characterization of perylene and 1,7-diazaperylene in dilute solution, solutions with a concentration of 10^{-5} M in chloroform were prepared. For characterization of solid films, thin films on glass were prepared by physical vapor deposition technique or by spincoating at 800 rpm from ca. 2 mg/mL solutions in chloroform or toluene/acetone (ratio 4 : 1).

Dielectric Spectroscopy

The impedance spectroscopy investigations were performed in the frequency range spanning from 10 kHz to 1 mHz for both perylene and 1,7'-diazaperylene in metal-insulator-metal configuration with 80 nm thick bottom and top aluminum electrodes respectively, deposited by physical vapor deposition technique. The instrument employed for the dielectric measurements was a Novocontrol Broadband Dielectric / Impedance Spectrometer (Novocontrol Technologies GmbH).

OFETs Fabrication

The architecture of the OFET device employed for this study involved a staggered bottom gate-top contact design. The design comprised a bilayer inorganic dielectric (aluminum oxide, AlOx) and a thin capping layer of organic dielectric (either tetratetracontane, TTC, or 1,7-diazaperylene). The thickness of the aluminum gate electrodes that were subsequently anodized was 80 nm for all the OFET devices fabricated in this study. The aluminum oxide was grown electrochemically by employing a previously reported recipe[19] that was optimized over the years in our laboratories.[20,21] The setup comprised a current-voltage source meter, Keithley 4ZA4. The aluminum used for evaporation of the gate electrode had a purity of 99.999% (ChemPUR GmbH) and the respective gate electrode layer was evaporated at a fast rate of ~4–5 nm/sec. The anodization voltage of this study was set to 10 V. The source and drain electrodes were aluminum for C_{60} and gold for pentacene respectively, and the channel dimensions were length, L = 25 µm and width, W = 2 mm (see Figure 1). The OFETs were measured with the aid of a probe station in glove box, under nitrogen atmosphere.

Results and Discussion

The chemical structures of 1,7-diazaperylene (1) and the chemically related compound, perylene (2) are shown in the schematic below.

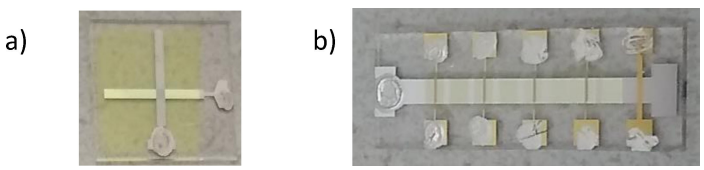

Figure 1. a) Photograph of a metal-insulator-metal structure with 1,7-diazaperylene sandwiched between two pairs of aluminum electrodes; b) Photograph of the OFET structure employed in this work displaying the bottom gate electrode, the patterned diazaperylene semiconductor, and the 4 pairs of source and drain electrodes. The mask allowed also the patterning of a MIM structure (yellow electrode on the far right of the photograph) necessary for the measurement of the specific capacitance of the field effect transistor. The electrode contacts were decorated with silver paste for the measurement purposes.

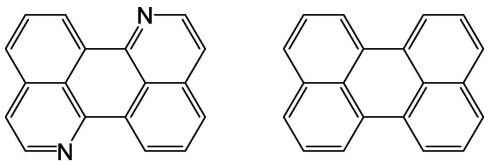

(1) (2)

In this work we scrupulously purified 1,7-diazaperylene via train sublimation method[21] and pursued a thorough materials characterization of this compound in its high purity form. After two rounds of sublimation for perylene and 1,7-diazaperylene respectively, the purity of the investigated compounds became (presumably) significantly higher than 99%. We further looked into the possibility of this compound having a useful functionality in field effect transistors and solar cells. We analyzed the 1,7-diazaperylene by cyclic voltammetry (CV), photoluminescence spectroscopy (PL), UV-Vis absorption spectroscopy (UV-Vis), and impedance spectroscopy (IS). We compared the results of these investigations with the respective data recorded for perylene, a molecule that is already established as p-type organic semiconductor.[22]

Figure 2 presents the CV spectra of 1,7-diazaperylene and perylene respectively solubilized in acetonitrile (MeCN). The CV reveals that perylene has a reversible reduction peak at −1.43 V and a reversible oxidation peak at +1.26 V, similar to observations of the litereture.[17] At more anodic potentials, a further irreversible oxidation takes place at +1.78 V. In comparison to perylene, the full CV cycle in case of 1,7-diazaperylene appears to be anodically shifted. A reversible, first reduction peak at −1.00 V occurs followed by a second reduction peak at −1.48 V. A first oxidation peak was observed at +1.67 V followed by a second oxidation peak at +2.07 V, which both appear to be irreversible. Comparing the onset values of the reduction and oxidation gives an electrochemical band gap of 2.51 eV for perylene and 2.59 eV for 1,7-diazaperylene. This smaller band-gap of perylene in comparison with the 1,7-diazaperylene is in agreement with the optical absorption spectra.

Figure 3 shows in the panel a) the absorbance and photoluminescence (PL) spectra of perylene and 1,7-diazaperylene in dilute (10^{-5} M) chloroform solution, and in the panel b) the photoluminescence excitation (PLE) and PL spectra of both materials in solid films deposited on glass by physical vapor deposition. In dilute chloroform solution both molecules show electronic transitions to different vibrational levels with increasing peak intensities towards lower energy and a very small Stokes shift of the emission spectra which are characteristic footprint of perylene derivatives.[3,17,23–26] In solution, 1,7-diazaperylene displays PL transitions at wavelengths of 447, 476, 508 and 545 nm. Both the absorption and the PL bands of 1,7-diazaperylene show a small shift (*ca.* 4 nm) towards higher wavelengths as compared to the bands of perylene. This small red-shift can be attributed to slightly changed electronic properties due to the substitution of two carbon atoms of the aromatic system by nitrogen in diazaperylene.[2,3,27]

The thin films of both materials show significantly different positions and shapes of the absorption and PL bands as compared to their chloroform solutions. The fluorescence of both materials is strongly red-shifted with an emission maximum at 612 nm for 1,7-diazaperylene and 610 nm for perylene. Besides the small difference of the emission maxima, the shapes of the PL spectra of both materials in the thin film are almost identical. Furthermore, the PL spectra

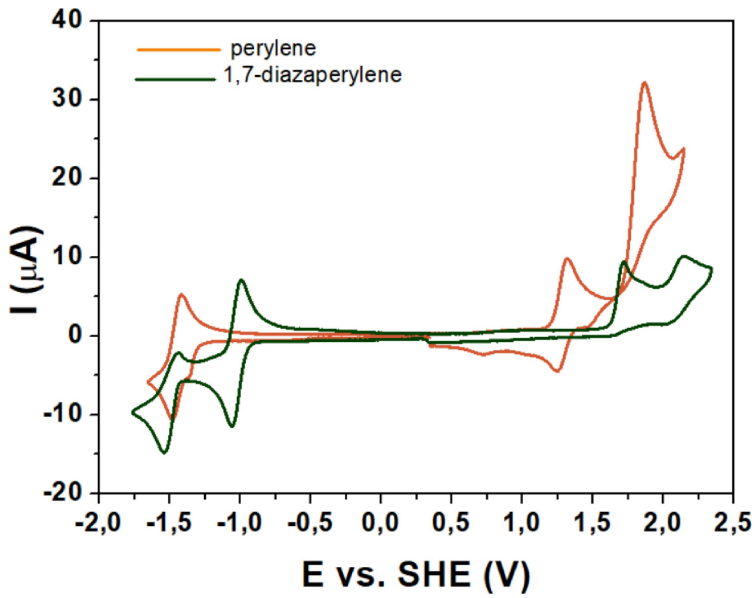

Figure 2. Cyclic voltammetry (CV) scans of perylene (orange color) and 1,7-diazaperylene (green color).

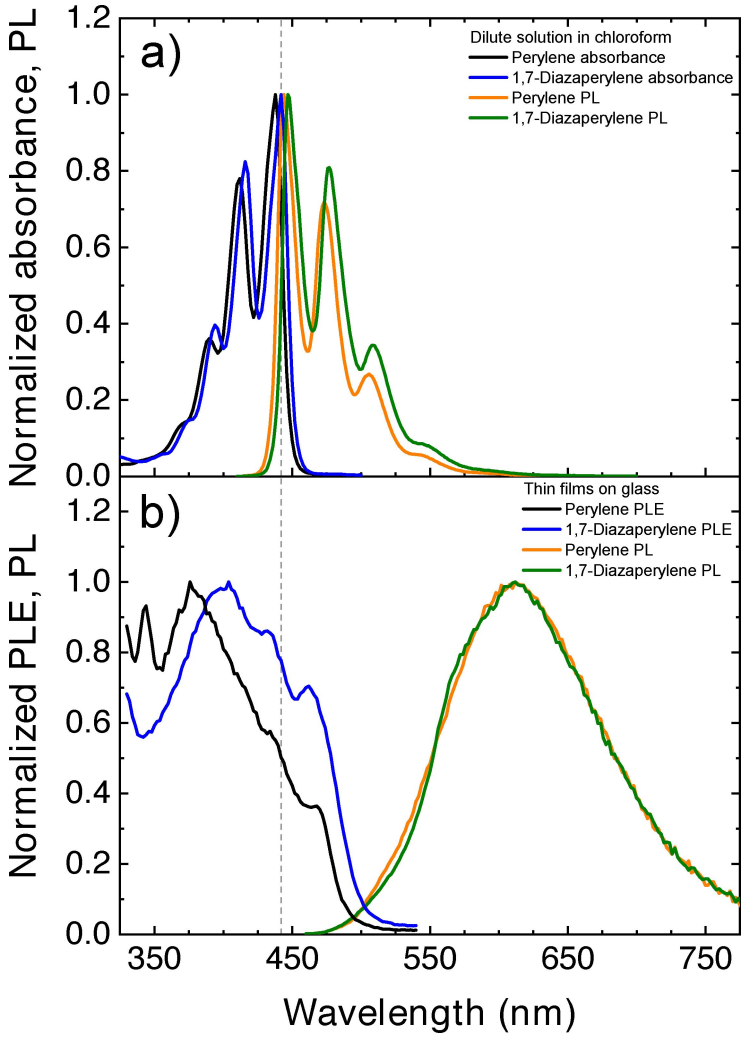

Figure 3. a) Normalized absorbance and photoluminescence (PL) spectra of perylene and 1,7-diazaperylene measured in 10^{-5} M chloroform solution. b) Photoluminescence excitation (PLE) and PL spectra of solid films of perylene and 1,7-diazaperylene deposited on glass. The dashed grey line marks the spectral position of the main absorption peak of 1,7-diazaperylene in solution and is included as a guide for the eye for comparison of the spectra.

show a broad shape, large Stokes shift and absence of the typical vibrational structure observed for the monomeric molecules in dilute solution. These observations suggest a strong excimer formation in the solid films of both molecules as has been previously reported for perylene crystals and thin films.[28,29]

In comparison to the dilute solutions, the absorption bands of perylene and 1,7-diazaperylene show a spectral shift and broadening in the solid films as evident from the PLE spectra. For perylene the spectrum shows the emergence of a relatively weak lower energy absorption band at 468 nm. Much more pronounced, however, is the hypsochromic shift of the absorption maximum to 380 nm and the emergence of an additional absorption band at 344 nm. This can be related to a strong H-aggregate formation in the film.[30,31] For perylene, this strong aggregation can be attributed to the occurrence of closely stacked dimers in the molecular packing in the α-perylene crystalline form[28,32] which has also been reported for thin films of this material.[29] For the 1,7-diazaperylene thin film, a similar red-shifted absorption band and shift of the maximum absorption intensity towards shorter wavelengths as compared to the chloroform solution can be observed. In comparison to the perylene thin film, 1,7-diazaperylene shows a much lower magnitude of the hypsochromic shift and a significantly higher relative intensity of the lower energy absorption bands. This suggests a lower tendency of this material towards H-aggregate formation. This is further corroborated by the differences in molecular packing as shown by comparison of the crystal structures reported for perylene[28,33,34] and 1,7-diazaperylene.[14] While perylene in its α form shows an arrangement of closely spaced slipped-parallel dimers, no such dimeric arrangement was observed for

1,7-diazaperylene. The strong π-π interaction in H-aggregated molecules typically strongly benefits the charge transport properties of the material.[35,36] Significant differences in the aggregation behavior of the investigated perylene derivatives may thus relate to differences in their performance as active materials in photovoltaics and OFETs.

Since the isolation of two different modifications of solid 1,7-diazaperylene has been reported earlier,[14] the optical properties of 1,7-diazaperylene thin films processed from different solutions were investigated to characterize a possible occurrence and influence of different modifications in solid films. The PLE and PL spectra of films prepared by spincoating from solutions of 1,7-diazaperylene in chloroform and in a toluene/acetone mixture (volumetric ratio 4 : 1) are shown in Figure 4. The PLE spectra of both films show a similar shape and conform very well to the PLE spectrum of the thin film deposited by PVD (see Figure 3). This suggests a similar ground-state aggregation behavior of 1,7-diazaperylene in films deposited from chloroform, toluene/acetone or by PVD, respectively. However, the films deposited from chloroform and toluene/acetone display a clearly different spectral position and shape of their fluorescence spectra. The PL spectrum of the film deposited from chloroform shows an emission maximum at 610 nm and conforms well to the PL measured for the 1,7-diazaperylene film deposited by PVD. The emission spectrum of the thin film deposited from toluene/acetone shows a lower Stokes shift with an emission maximum at 580 nm and a pronounced shoulder centered at 546 nm. This suggests a lower degree of excimer formation as compared to the films processed from chloroform. The differences in the PL spectra could be attributed to the formation of different modifications of 1,7-diazaperylene in thin films processed from different solvents. Slight differences in the arrangement of the molecules in these solid modifications may show a similar π-π stacking in the ground state but a significantly changed excimer formation behavior, as was observed for pyrene derivatives when crystallized from different solvents.[37,38] Ge *et al.* attributed this observation to a dissimilar overlap area of the pyrene units in the different crystalline modifications.[37] The PL spectra observed for 1,7-diazaperylene suggest that the material has an identical excimer formation behavior in the vapor-deposited thin film and in the film solution-processed from chloroform.

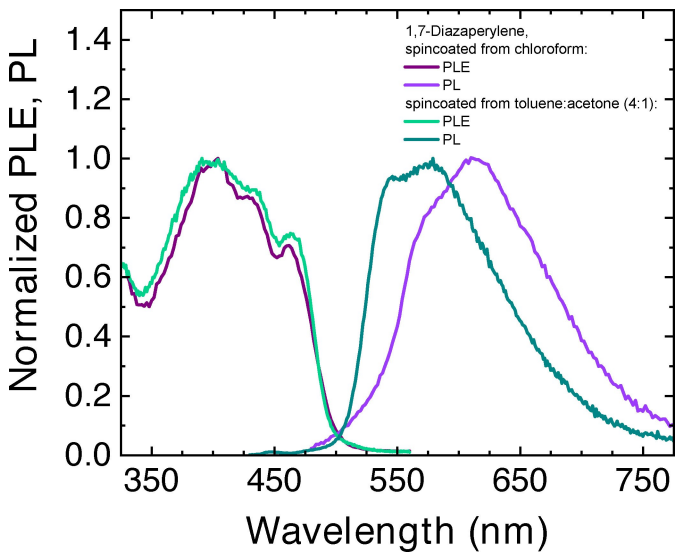

Figure 4. Normalized photoluminescence excitation (PLE) and photoluminescence (PL) spectra of 1,7-diazaperylene films spin coated on fused quartz from solutions in chloroform and in a 4 : 1 toluene/acetone mixture.

The energetic HOMO-LUMO difference corresponding to the gap energy of isolated molecules is indicated by the absorption and fluorescence spectra in diluted solution (there are pure pi-pi* transitions in both cases, *i.e.* perylene and 1,7-diazaperylene, because the lone pairs are energetically below the HOMO level); this is shown in Figure 3a where the electronic transitions for 1,7-diazaperylene are more bathochromic shifted (lower energy) than for perylene. This is still true for solid films (see Figure 3b), although there are additional exciton couplings in the solids because of the proximity of the densely packed chromophores. There may be several reasons, (two of them are listed below) for the lower HOMO-LUMO gap of perylene which should not be discussed in detail unless they are supported by high-level quantum chemical calculations: (i) there are unfavorable interactions in perylene such as those caused by a slight sterically-induced twisting and a repulsion of the filled orbitals in the formal two combined naphthalene units. This is indicated by the two elongated bonds between the units being more single bonds than aromatic double bonds; (ii) 1,7-diazaperylene might be slightly favored because of minor steric repulsion and stabilization by antiparallel dipoles cause by the electron withdrawing nitrogen atoms. On the other hand, the effects in the UV/Vis spectra are comparably small.

Clarifying the major contributor to the HOMIO-LUMO level difference in perylene vs. 1,7-diazaperylene is not easy since DFT calculations are known to give rather useful results for the interaction of orbitals, moderate results for electrostatic interactions and rather poor results for steric interactions of more distant parts of molecules (for example, an incorrect orthogonal geometry is obtained for biphenyl). Having these said, we find indeed the electrochemical results rather puzzling because the reduction of perylene requires −1.43 V and its oxidation +1.26 V resulting in a difference of 2.69 V; whereas the respective values for 1,7-diazaperylene were −1.00 V and +1.67 V, causing a difference of 2.67 V. This slightly smaller value is consistent with the slightly more bathochromic (lower energy) absorption and fluorescence of 1,7-diazaperylene. Moreover, the shift to more positive values for reduction and oxidation for 1,7-diazaperylene is in accordance with the electron depletion by the two more electronegative nitrogen atoms

Impedance spectroscopy is very informative tool used to explain the processes that occur at interfaces between two different layers of materials that lead to changes in physical

properties of the system. Impedance spectroscopy helps also understanding changes in the electrical properties of the system by studying the effect of polarization on the electrical conductivity alteration.[39–43] Impedance spectroscopy investigation on thin films of perylene and 1,7-diazaperylene is displayed in Figure 5. Both thin films of vacuum processed perylene (~150 nm) and 1,7-diazaperylene (~125 nm) were sandwiched between aluminum electrodes fabricated via physical vacuum deposition. The impedance measurements were carried out with the aid of a Novocontrol Impedance analyzer in ambient air. With each scan from 10 kHz to 1 mHz lasting 8 hours, it is visible in the Figure 5 that oxidation of the two thin films occurs, an event that has as a typical characteristic a decrease in time of both the capacitance of the film and the loss angle (highlighted by arrows on the respective graphs). The oxidation event makes the films lose their semiconductor properties and turns them into better dielectrics instead. Nevertheless, in the case of perylene the oxidation event[44,45] stabilizes so that the capacitance and the loss angle reach a stable value after 3 days exposure to oxygen, whereas the respective event continues without stoppage for the 1,7-diazaperylene for the entire extent of the measurement, *i.e.* 6 days.

Our attempts to fabricate photovoltaic devices with 1,7-diazaperylene in planar diode configurations, a geometry reported originally by C. W. Tang[46] did not produce the desired results. With this respect, 1,7-diazaperylene did not produce any photocurrent neither when it was employed as a donor (interfaced with PTCDI), or as an acceptor (*i.e.* interfaced with copper phthalocyanine or zinc phthalocyanine respectively). The attempt to utilize 1,7-diazaperylene as a homojunction semiconductor[47,48] (single material in a single layer, sandwiched between a pair of electrodes, *i.e.* anode, ITO + PEDOT-PSS, and cathode, *i.e.* either plain aluminum, Ca–Al or LiF–Al) also did not produce the expected results. In case when 1,7-diazaperylene was investigated as donor material, its thickness was 40 nm, and the acceptor layer's thickness (i.e. PTCDI) was 20 nm. In the opposite case when 1,7-diazaperylene was employed as acceptor (n-type material), its thickness was varied, from 30 nm to 10 nm, in successive batches. The respective devices did not have an electron transporting layer to face the top electrode.

We focused then our attention toward field effect transistors. We attempted to fabricate devices with 1,7-diazaperylene as an organic semiconductor on AlOx-TTC inorganic-organic composite dielectric, but we did not record any transistor behavior, neither as n-type (capped by aluminum or silver source and drain electrodes) nor as p-type (capped by gold source and drain electrodes) respectively. We did not record any semiconductor characteristics for the respective material either when deposited slow or fast in several batches. With this respect we kept the deposition rate constant for each batch but we deposited the 1,7-diazaperylene at rates starting with less than 1 Å/sec. and finishing at 8 nm/sec. in successive batches), thinking that this material is morphology and growth model sensitive as it is the case of tetracene for example, where deposition rates in excess of 0.5 nm/sec. are required in order to raise the semiconductor properties.[49,50] However, our efforts did not pay dividends, and the perylene derivative employed in this study did not show any semiconducting behavior.

Nevertheless, corroborating these findings with the information offered by impedance spectroscopy relative to the suitability of 1,7-diazaperylene as dielectric material, we proceeded by fabricating OFET devices with pentacene and fullerene (C_{60}) semiconductors and 1,7-diazaperylene as thin dielectric capping layer on AlOx inorganic dielectric. Employing 1,7-diazaperylene as capping layer for electrochemically grown aluminum oxide inorganic dielectric, we put its performance in context of a classic, well established capping layer, tetratetracontane (TTC, $C_{44}H_{90}$). We fabricated our first batch of OFET devices with C_{60} semiconductor directly deposited on AlOx, in effect without any passivating layer (see Figure 6). The OFET device displays a clear print of unpassivated AlOx, where the strong dipoles of the inorganic dielectric generate a very large hysteresis in the transfer

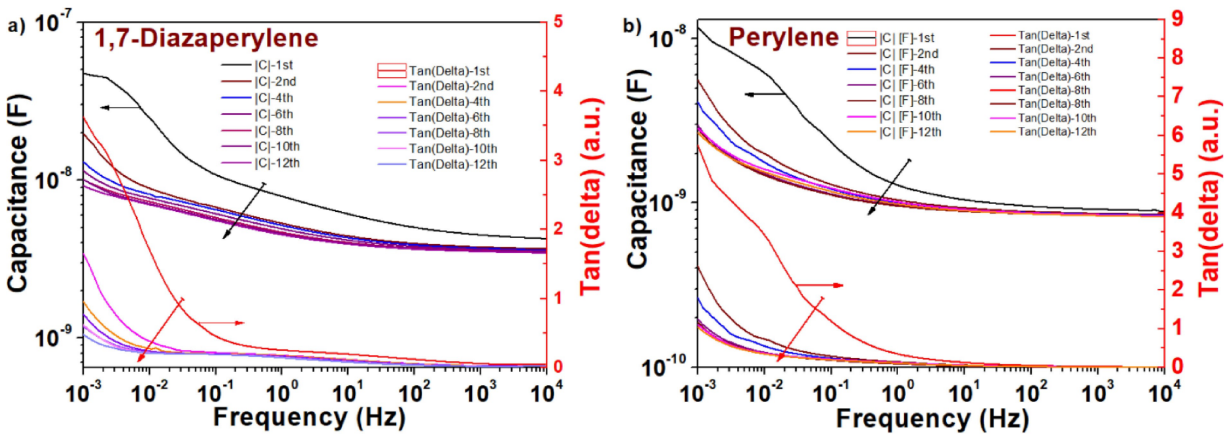

Figure 5. Impedance spectroscopy of a) 1,7-diazaperylene and b) perylene in a frequency window spanning 10 kHz to 1 mHz.

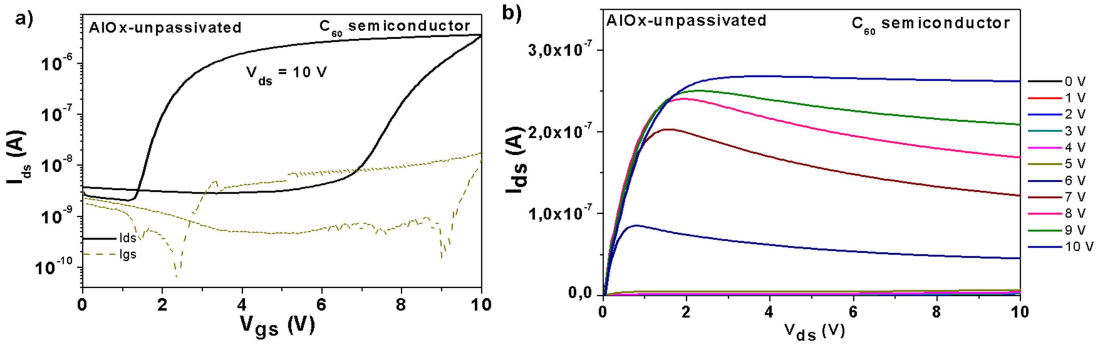

Figure 6. Unpassivated AlOx + C_{60} semiconductor. a) transfer characteristics; b) output characteristics. The specific capacitance of the dielectric layer was C_{0d} = 468.6 nF/cm^2 and the electron field effect mobility $\mu_e = 1.2 \times 10^{-2}$ cm^2/Vs.

characteristic, as well as a lack of full saturation (seen clearly in the output characteristic). The respective finding demonstrated the importance of finding a good capping layer for the AlOx when interfacing it with fullerene.

Devices with 1,7-diazaperylene and TTC capping layers respectively on AlOx and C_{60} semiconductor are presented in Figure 7. Both devices display minimal hysteresis, however the 1,7-diazaperylene capping layer generated a superior interface with C_{60} that resulted in a higher electron mobility, *i. e.* 1.2 $\times 10^{-3}$ cm^2/Vs for AlOx-1,7-diazaperylene vs. 3.3 $\times$ 10^{-4} cm^2/Vs for AlOx-TTC.

Devices with pentacene semiconductor deposited on TTC and 1,7-diazaperylene capping layer are displayed in Figure 8. In a similar behavior with the study of C_{60} deposited on the

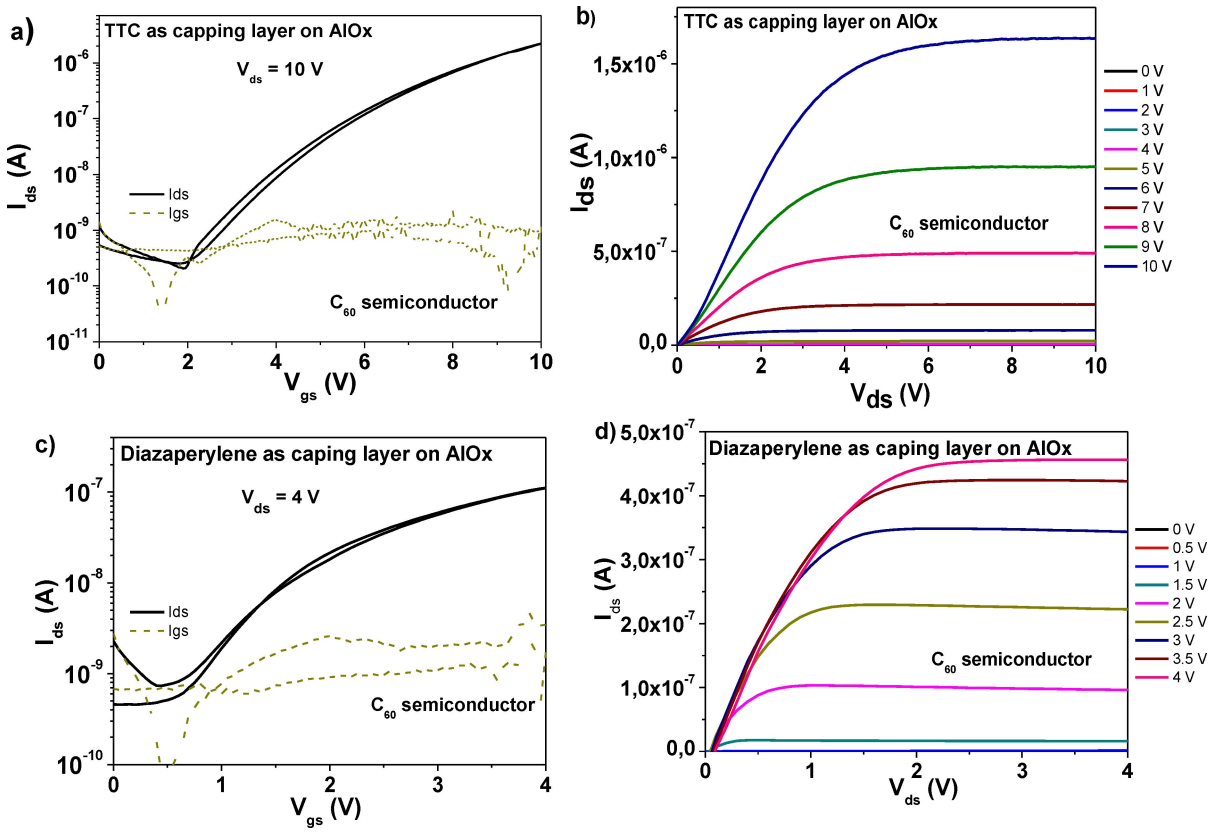

Figure 7. TTC as capping layer on AlOx + C_{60} semiconductor: a) transfer and b) output characteristics. The measured specific capacitance of the OFET device was C_{0d} = 396.1 nF/cm^2. The calculated field effect mobility was $\mu_e = 3.3 \times 10^{-4}$ cm^2/Vs; Diazaperylene as capping layer on AlOx 10 V + C_{60} semiconductor: c) transfer and d) output characteristics. The measured specific capacitance of the OFET device was C_{0d} = 409.8 nF/cm^2. The calculated field effect mobility was $\mu_e = 1.2 \times 10^{-3}$ cm^2/Vs.

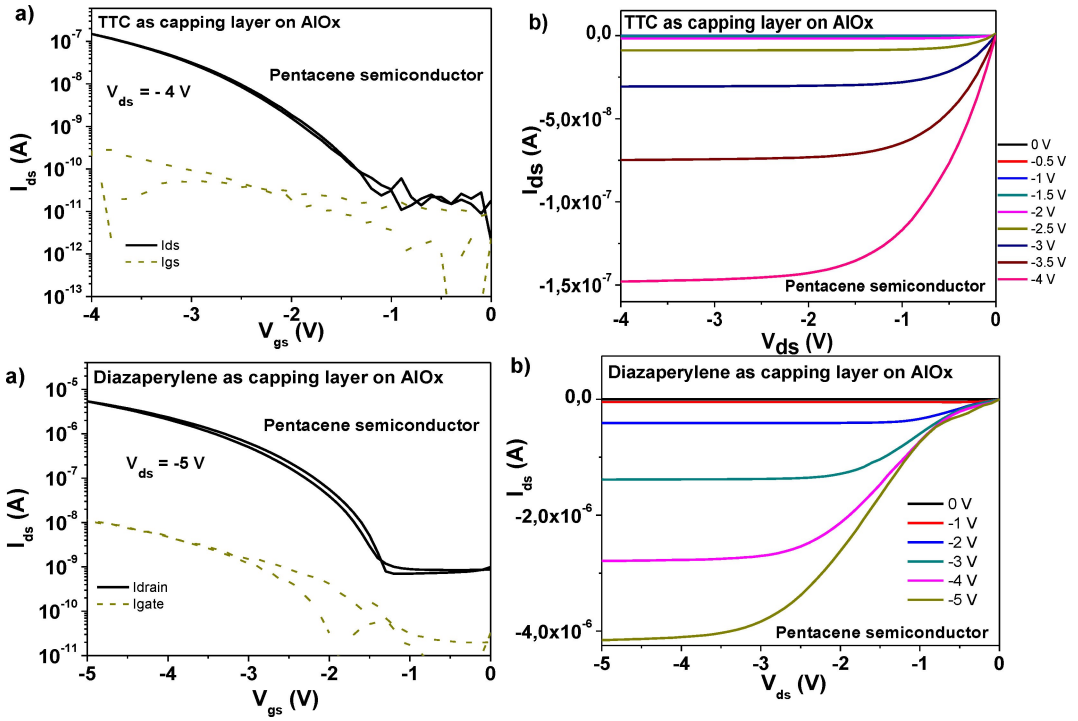

Figure 8. TTC as capping layer on AlOx + pentacene semiconductor: a) transfer characteristics and b) output characteristics. The specific capacitance of the OFET device was $C_{0d} = 399.3$ nF/cm^2. The calculated field effect mobility was $\mu_h = 3.8 \times 10^{-3}$ cm^2/Vs; 1,7-diazaperylene as capping layer on AlOx + pentacene semiconductor: c) transfer characteristics and d) output characteristics. The specific capacitance of the OFET device was $C_{0d} = 413.5$ nF/cm^2. The calculated field effect mobility was $\mu_h = 1 \times 10^{-2}$ cm^2/Vs.

respective capping layers, also the devices with 1,7-diazaperylene generates high hole field effect mobility in pentacene semiconductor as compared to similar devices featuring TTC as capping layer (1×10^{-2} cm^2/Vs vs. 3.8×10^{-3} cm^2/Vs).

We finished our OFETs studies by investigating the performance of perylene semiconductor on aluminum oxide capped by TTC vs. 1,7-diazaperylene. In a convincing fashion (see Figure 9), and in line with the previous observations involving C_{60} and pentacene semiconductors, also in the case of perylene semiconductor, the hole field effect mobility was higher when perylene was grown on 1,7-diazaperylene 3×10^{-3} cm^2/Vs than on TTC, i. e. 3×10^{-4} cm^2/Vs.

Conclusions

In this study we performed a thorough material characterization of 1,7-diazaperylene via multiple techniques, and looked for the applicability of this perylene derivative in organic electronic devices. We could not obtain any photovoltaic effect behavior in planar diodes where 1,7-diazaperylene was employed both as a donor (in combination with PTCDI) as well as an acceptor (in combination with copper phthalocyanine or zinc phthalocyanine respectively). All our efforts to extract a semiconductor behavior in field effect transistors also proved unsuccessful, despite varying several deposition and fabrication parameters. We ultimately focused our attention into demonstrating the dielectric properties of 1,7-diazaperylene. Indeed, this material seems to be an exception to the rule in the class of perylene derivatives, in the sense that it behaves as an insulator. The reason for this behavior is presumably generated by the differences in crystal structure and growth (aggregation in thin film) of 1,7-diazaperylene and perylene respectively, a topic that requires careful investigation. This explanation is corroborated by the differences in the optical absorption properties of the thin films of the two materials which strongly suggest a significantly weaker H-aggregation in 1,7-diazaperylene as compared to perylene. Finally, the dielectric behavior of 1,7-diazaperylene recommends this material as a thin capping layer for the passivation of inorganic dielectrics employed in the fabrication of organic field effect transistors, with performance similar to other dielectrics like vacuum processed polyethylene, pentacontane, waxes, cellulose, trimethylsilyl cellulose (TMSC), or natural resins or gums.[51–55]

Data Availability Statement

The data that support the findings of this study are available from the corresponding author upon reasonable request.

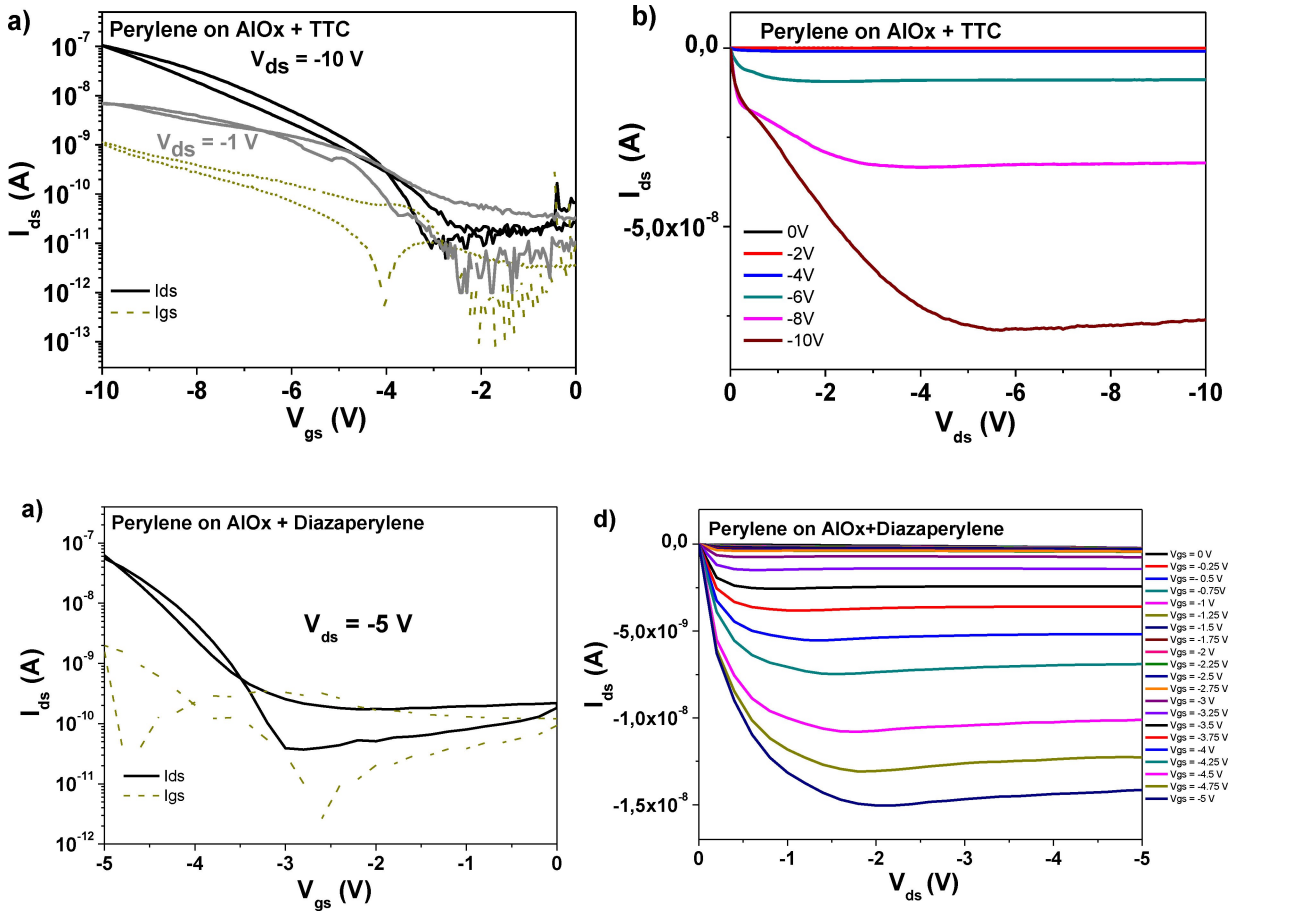

Figure 9. a) and b) transfer and output characteristics of perylene on AlOx+TTC. The specific capacitance of the OFET was C_{0d} = 397.5 nF/cm^2. The calculated field effect mobility of the perylene semiconductor was $\mu_h = 3.6\times10^{-4}$ cm^2/Vs; c) and d) transfer and output characteristics of perylene on AlOx+1,7-diazaperylene dielectric. The specific capacitance of the OFET was C_{0d} = 409.8 nF/cm^2. The calculated field effect mobility of the perylene semiconductor was $\mu_h = 3.2\times10^{-3}$ cm^2/Vs.

References

[1] J. T. Markiewicz, F. Wudl, *ACS Appl. Mater. Interfaces* **2015**, *7*, 28063.
[2] C. Naumann, H. Langhals, *Chem. Ber.* **1990**, *123*, 1881–1887.
[3] L. B. -Å Johansson, J. Karolin, H. Langhals, S. Reichherzer, N. von Füner, K. J. Polborn, *J. Chem. Soc. Faraday Trans.* **1993**, *89*, 49–54.
[4] M. Alipour, S. Damiri, *J. Chem. Phys.* **2020**, *152*, 204301.
[5] T. Xiong, R. Wlodarczyk, P. Saalfrank, *Chem. Phys.* **2018**, *515*, 728–736.
[6] Z. C. Wong, W. Y. Fan, T. S. Chwee, M. B. Sullivan, *Phys. Chem. Chem. Phys.* **2017**, *19*, 21046–21057.
[7] L. Ryderfors, E. Mukhtar, L. B. Johansson, *J. Phys. Chem. A* **2008**, *112*, 5794–5803.
[8] A. Habenicht, J. Hjelm, E. Mukhtar, F. Bergstrom, B.-A. L Johansson, *Chem. Phys. Lett.* **2002**, *354*, 367–375.
[9] M. Cyranski, T. M. Krygowski, *Tetrahedron* **1996**, *52*, 13795–13802.
[10] S. A. Tucker, W. F. Jr Acree, M. J. Tanga, S. Tokita, K. Hiruta, H. Langhals, *Appl. Spectrosc.* **1992**, *46*, 229–235.
[11] O. E. Polansky, M. Zander, I. Motoc, *Kosmophysik* **1983**, *38A*, 196–199.
[12] A. Hirono, H. Sakai, T. Hasobe, *Chem. Anal.* **2019**, *14*, 1754–1762.
[13] D. S. Baranov, M. N. Uvarov, M. S. Kazantsev, E. A. Mostovich, E. M. Glebov, Y. V. Gatilov, L. V. Kulik, *Dyes Pigm.* **2017**, *136*, 707–714.
[14] H. Langhals, S. Reichherzer, P. Mayer, K. Polborn, *Synthesis* **2021**, *53*, 713–722.
[15] V. V. Jarikov, U. S. Pat. Appl. Publ. **2004**, US 20040076853 A1 20040422.
[16] W. Toyama, T. Hayano, Matsuura, Jpn. Kokai Tokkyo Koho **2000**, JP 2000231987 A 20000822.
[17] A. Hirono, H. Sakai, S. Kochi, T. Sato, T. Hasobe, *J. Phys. Chem. B* **2020**, *124*, 9921–9930.
[18] N. G. Connelly, W. E. Geiger, *Chem. Rev.* **1996**, *96*, 877–910.
[19] L. A. Majewski, M. Grell, S. D. Ogier, J. Veres, *Org. Electron.* **2003**, *4*, 27–32.
[20] M. Irimia-Vladu, P. A. Troshin, M. Reisinger, G. Schwabegger, M. Ullah, R. Schwödiauer, A. Mumyatov, M. Bodea, J. W. Fergus, V. F. Razumov, H. Sitter, S. Bauer, N. S. Sariciftci, *Org. Electron.* **2010**, *11*, 1974–1990.
[21] C. Yumusak, N. S. Sariciftci, M. Irimia-Vladu, *Mater. Chem. Front.* **2020**, *4*, 3678–3689.

[22] H. Akamasu, H. Inokuchi, Y. Matsunaga, *Nature* **1954**, *173*, 168–169.
[23] S. A. Tucker, H. Darmodjo, W. E. Acree, Jr., M. Zander, E. C. Meister, M. J. Tanga, S. Tokita, *Appl. Spectrosc.* **1992**, *46*, 1630–1635.
[24] S. A. Tucker, W. E. Jr Acree, C. Upton, *Appl. Spectrosc.* **1993**, 47, 201–206.
[25] M. Tange, T. Okazaki, Z. Liu, K. Suenaga, S. Iijima, *Nanoscale* **2016**, *8*, 7834–7839.
[26] A. Sanguineti, M. Sassi, R. Turrisi, R. Ruffo, G. Vaccaro, F. Meinardia, L. Beverina, *Chem. Commun.* **2013**, *49*, 1618–1620.
[27] T. Sander, H.-G. Loehmannsroeben, H. Langhals, J. Photochem, *J. Photochem. Photobiol. A Chem.* **1995**, *86*, 103–108.
[28] J. Tanaka, *Bull. Chem. Soc. Jpn.* **1963**, *36*, 1237–1249.
[29] W. Ni, L. Sun, G. G. Gurzadyan, *Sci. Rep.* **2021**, *11*, 5220.
[30] F. C. Spano, *Acc. Chem. Res.* **2010**, *43*, 429–439.
[31] N. J. Hestand, F. C. Spano, *Chem. Rev.* **2018**, *118*, 7069.
[32] A. Datta, S. Mohakud, S. K. Pati, *J. Mater. Chem.* **2007**, *17*, 1933–1938.
[33] D. M. Donaldson, J. M. Robertson, J. White, *Proc. Roy. Soc. A* **1953**, *220*, 311–321.
[34] A. Camerman, J. Trotter, *Proc. Roy. Soc. A* **1964**, *279*, 129–146.
[35] V. Coropceanu, J. Cornil, D. A. da Silva Filho, Y. Olivier, R. Silbey, J.-L. Bredas, *Chem. Rev.* **2007**, *107*, 926–952.
[36] S. Ma, S. Du, G. Pan, S. Dai, B. Xu, W. Tian, *Aggregate* **2021**, *2*, e96.
[37] Y. Ge, Y. Wen, H. Liu, T. Lu, Y. Yu, X. Zhang, B. Li, S. Zhang, W. Li, B. Yang, *J. Mater. Chem. C* **2020**, *8*, 11830–11838.
[38] W. Jiang, Y. Shen, Y. Ge, C. Zhou, Y. Wen, H. Liu, H. Liu, S. Zhang, P. Lu, B. Yang, *J. Mater. Chem. C* **2020**, *8*, 3367–3373.
[39] M. Egginger, M. Irimia-Vladu, R. Schwödiauer, A. Tanda, I. Frischauf, S. Bauer, N. S. Sariciftci, *Adv. Mater.* **2008**, *20*, 1018–1022.
[40] A. H. Alami, K. Aokal, D. Zhang, A. Taieb, M. Faraj, A. Alhammadi, J. M. Ashraf, B. Soudan, J. El Hajjar, M. Irimia-Vladu, *Int. J. Energy Res.* **2019**, *43*, 5824–5833.
[41] M. Irimia-Vladu, J. W. Fergus, *Synth. Met.* **2006**, *156*, 1396–1400.
[42] M. Irimia-Vladu, N. Marjanovic, M. Bodea, G. Hernandez-Sosa, A. Montaigne Ramil, R. Schwödiauer, S. Bauer, N. S. Sariciftci, F. Nüesch, *Org. Electron.* **2009**, *10*, 408–415.
[43] A. Petritz, A. Wolfberger, A. Fian, T. Griesser, M. Irimia-Vladu, B. Stadlober, *Adv. Mater.* **2015**, *27*, 7645–7656.
[44] A. Zinke, K. J. v Schieszl, F. Hanus, *Monatsh. Chem.* **1936**, *67*, 196–202.
[45] A. Zinke, E. Zeschko, R. Ott, *Monatsh. Chem.* **1960**, *91*, 445–449.
[46] C. W. Tang, *Appl. Phys. Lett.* **1986**, *48*, 183–185.
[47] S. Dunst, E. Karner, M. E. Coppola, G. Trimmel, M. Irimia-Vladu, *Monatsh. Chem.* **2017**, *148*, 863–870.
[48] E. D. Glowacki, L. Leonat, M. Irimia-Vladu, R. Schwödiauer, M. Ullah, H. Sitter, S. Bauer, N. S. Sariciftci, *Appl. Phys. Lett.* **2012**, *101*, 023305.
[49] F. Cicoira, C. Santato, F. Dinelli, M. Murgia, M. A. Loi, F. Biscarini, R. Zamboni, P. Heremans, M. Muccini, *Adv. Funct. Mater.* **2005**, *15*, 375–380.
[50] E. D. Glowacki, M. Irimia-Vladu, M. Kaltenbrunner, J. Gąsiorowski, M. S. White, G. Romanazzi, G. P. Suranna, P. Mastrorilli, T. Sekitani, S. Bauer, T. Someya, L. Torsi, N. S. Sariciftci, *Adv. Mater.* **2013**, *25*, 1563–1569.
[51] B. Stadlober, E. Karner, A. Petritz, A. Fian, M. Irimia-Vladu, *45th European Solid-State Device Research Conference (ESSDERC)* **2015**, *0–17*, DOI: 10.1109/ESSDERC.2015.7324701.
[52] A. Petritz, A. Fian, E. D. Głowacki, N. S. Sariciftci, B. Stadlober, M. Irimia-Vladu, *Phys. Status Solidi RRL* **2015**, *9*, 358–361.
[53] A. Petritz, A. Wolfberger, A. Fian, M. Irimia-Vladu, A. Haase, H. Gold, T. Rothländer, T. Grießer, B. Stadlober, *Appl. Phys. Lett.* **2013**, *103*, 191–1.
[54] Y. Kanbur, M. Irimia-Vladu, E. D. Głowacki, G. Voss, M. Baumgartner, G. Schwabegger, L. Leonat, M. Ullah, H. Sarica, S. Erten-Ela, R. Schwödiauer, H. Sitter, Z. Küçükyavuz, S. Bauer, N. S. Sariciftci, *Org. Electron.* **2012**, *13*, 919–924.
[55] M. Baumgartner, M. E. Coppola, N. S. Sariciftci, E. D. Glowacki, S. Bauer, M. Irimia-Vladu, "Emerging "green" materials and technologies for electronics", pages 1–53, in "Green Materials for Electronics", M. Irimia-Vladu, E. D. Glowacki, N. S. Sariciftci, S. Bauer Edt., **2018** Wiley-VCH Verlag GmbH & Co. KGaA 10.1002/9783527692958.

Manuscript received: November 14, 2021
Revised manuscript received: December 31, 2021
Version of record online: January 20, 2022